Monte Carlo simulations of the pseudospin model of RbSCN

1999 J. Phys.: Condens. Matter 11 2449

(http://iopscience.iop.org/0953-8984/11/11/015)

J. Phys.: Condens. Matter **11** (1999) 2449–2458. Printed in the UK PII: S0953-8984(99)99114-2

Monte Carlo simulations of the pseudospin model of RbSCN

Z Łodziana†‡, W Schranz† and A Fuith†

† Institute of Experimental Physics, University of Wien, Strudlhofgasse 4, 1090 Wien, Austria
‡ Institute of Nuclear Physics, ulica Radzikowskiego 152, 31-342 Kraków, Poland

Received 10 November 1998

Abstract. The microscopic Ising-like model of the order–disorder phase transition in improper ferroelastic crystals is presented. For such a system, the spin–strain coupling can be written in terms of four-spin interactions. Three-dimensional Monte Carlo simulation shows that for a certain strength of the four-spin interaction the system is close to the tricritical point. The calculated temperature dependence of the order parameter is in very good agreement with the experimental data for RbSCN. The results also show that the growth of the size of precursor clusters is suppressed when approaching T_c from below, whereas the order parameter susceptibility is increasing. This is in good agreement with the diffuse neutron scattering data on RbSCN and KSCN, which yield an increase of the diffuse intensity with increasing temperature below T_c, whereas its width remains constant throughout the whole ordered phase. These results show that elastic effects can stabilize the precursor clusters at the order–disorder phase transition below T_c.

1. Introduction

A great variety of molecular crystals exhibit order–disorder phase transitions with reorientations of molecules. As an example, in the case of the MSCN family (M = K, Rb, NH_4, ...) the phase transition is related to the ordering of linear semirigid SCN molecules, which are orientationally disoriented in the high-temperature phase [1]. The reorientation of SCN ions leads to the structural change from the low-temperature orthorhombic phase to the tetragonal phase above the transition temperature $T_c = 413$ K [1]. For that family of crystals a strong order parameter–strain coupling was found. The coupling is due to symmetry of the type $\eta^2\epsilon$. All MSCN crystals exhibit phase transitions which can be classified as first-order ones.

For solids the experimental investigations suggest that the strong coupling between the order parameter η (in MSCN, η is related to the orientation of SCN ions) and the lattice strains ϵ leads to a so-called strain-induced first-order phase transition. There are various ways to study this point. One approach comes from the Landau–Ginzburg theory, where the free energy is expanded in powers of the order parameter, and the gradient term of the spatial inhomogeneity of the order parameter is taken into account in successive applications of perturbation theory [2, 3]. Another approach comes from the mean-field theories, where microscopic models are subject to spatial averaging [3, 4]. The mechanism of these strain-induced first-order phase transitions, especially closely below T_c, is still not fully understood. For KSCN and RbSCN we have previously measured the temperature dependence of the diffuse neutron scattering intensity [5, 6]. We found an increase of the diffuse intensity when approaching T_c from below, whereas the width remains constant over the whole long-range-ordered phase. This effect contradicts the well known models, for which the temperature dependence of the diffuse intensity at the critical wave vector $I(q_c)$ and its width $\xi(r)^{-1}$ are

0953-8984/99/112449+10$19.50

coupled, i.e. $I_d(\bar{q}_c) \sim \xi^2(T)$. However, molecular dynamics simulations on a two-dimensional KSCN model have nicely reproduced this kind of behaviour [7, 8], and we concluded that the size of the precursor clusters is stabilized by the order parameter–strain interactions. To test this behaviour within a different approach, we performed three-dimensional Monte Carlo simulations of the pseudospin model of MSCN crystals and compared the results with the experimental data.

The outline of the paper is as follows. In section 2 we present the pseudospin formulation of the model of RbSCN, together with its computational adaptation. The main results of the simulations are presented in section 3, and a brief summary is given in section 4.

2. The model

2.1. The pseudospin model

The low-temperature phase of MSCN crystals has $Pbcm$ symmetry and contains four molecules per unit cell ($Z = 4$). The atoms form a layered structure, with layers aligned in (a, b) planes. As an example, the (a, b) plane projection of the orthorhombic unit cell of RbSCN is presented in figure 1. Below T_c the SCN molecules are orientationally ordered in the (a, b) plane as indicated by arrows in figure 1. They occupy two layers located at $c = \frac{1}{4}$ and $\frac{3}{4}$ respectively. The Rb atoms shown in figure 1 as circles are placed at $c = 0$ and $c = \frac{1}{2}$ respectively. In the high-temperature phase the unit cell changes to a body-centred-tetragonal one with $Z = 2$ and the SCN ions become orientationally disordered.

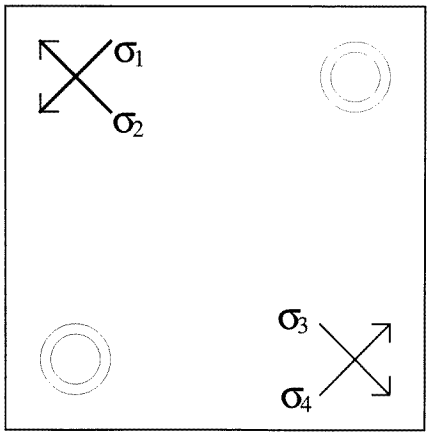

Figure 1. A sketch of the (a, b) plane of the unit cell of RbSCN. Arrows represent SCN ions and circles show the positions of Rb atoms.

The phase transition in KSCN and RbSCN crystals was previously successfully described in the language of the pseudospin model which was calculated in the mean-field approximation [1, 4]. The model consists of four spins σ^I ($I = 1, 2, 3, 4$) in each unit cell, representing four SCN ions. For such a system the compressible pseudospin Hamiltonian can be written in terms of volume-dependent interaction constants as proposed in [4]:

$$\mathcal{H} = -\frac{1}{2}\sum_{\alpha\beta}\sum_{R,R'}\left[J_{\alpha,\beta}(R, R') + J^{v}_{\alpha,\beta}(R, R')\epsilon_v\right]\sigma^{\alpha}(R)\sigma^{\beta}(R') + \frac{1}{2}\sum_{v} C_v\epsilon_v^2 \tag{1}$$

where $J_{\alpha,\beta}$ and $J^{v}_{\alpha,\beta}$ denote the coupling constants for spins, $\sigma^{\alpha}(R)$ is the spin variable, R is

the position vector of the spin σ^α, $\alpha, \beta = 1, 2, 3, 4$ label the spin variables within the unit cell, the C_ν are the elastic constants, and the ϵ_ν are the corresponding strains. Since in the high-temperature phase the spins 1, 4 and 2, 3 are perpendicular, there is no coupling between them and the corresponding interaction terms vanish, i.e. $J_{13} = J_{24} = J_{12} = J_{34} = 0$. Thus, neglecting elastic coupling, there are two independent sublattices in the system, i.e., σ^1–σ^4 and σ^2–σ^3. However, for nonzero order parameter–strain coupling, the two sublattices become unified. Assuming that in the equilibrium state all strains are homogeneous, one can use the equilibrium condition $\partial\mathcal{H}/\partial\epsilon = 0$, which leads to the following form of Hamiltonian (1):

$$\mathcal{H} = -\frac{1}{2}\sum_{\alpha,\beta}\sum_{R,R'} J_{\alpha,\beta}(R, R')\sigma^\alpha(R)\sigma^\beta(R') - \frac{1}{2}\sum_{\nu}\frac{1}{C_\nu}\left[\sum_{\alpha,\beta}\sum_{R,R'} J^\nu_{\alpha,\beta}(R, R')\sigma^\alpha(R)\sigma^\beta(R')\right]^2 \tag{2}$$

which, besides two-spin interactions, also includes the four-spin terms and the renormalized coupling constants.

2.2. The computational model

The present model used in our simulation (see figure 2) is a simple adaptation of the pseudospin model in which the interaction is limited to the nearest neighbours in each spin sublattice σ^I ($I = 1, 2, 3, 4$), i.e. nearest-neighbour interactions between σ^1–σ^4 and σ^2–σ^3, and the four-spin interactions within each unit cell are included. The Hamiltonian of the model reads

$$\mathcal{H} = -\sum_{\alpha=1,2,3,4}\left(\sum_{i,j,k} J\sigma^\alpha_{i,j,k}\sigma^\alpha_{i',j',k'}\right) - \sum_{\alpha,\alpha'}\left(\sum_{l,m,n} J_1\sigma^\alpha_{l,m,n}\sigma^{\alpha'}_{l',m',n'}\right) - \sum_{i,j,k} J_4\sigma^1_{i,j,k}\sigma^2_{i,j,k}\sigma^3_{i,j,k}\sigma^4_{i,j,k} \tag{3}$$

where the first sum runs over the nearest neighbours for each subspin system σ^α, and J denotes the interaction constant: $J = J_{\alpha\alpha}(R, R')$ ($\alpha = 1, 2, 3, 4$; $R = (i, j, k)$; R, R' run over nearest neighbours). The second sum represents the interaction between σ^1–σ^4 and σ^2–σ^3 with coupling constant $J_1 = J_{\alpha\beta}(R, R')$ ($\alpha\beta = 14, 23$; R, R' run over the nearest neighbours between different pairs of spins within each of the sublattices). The last term describes the

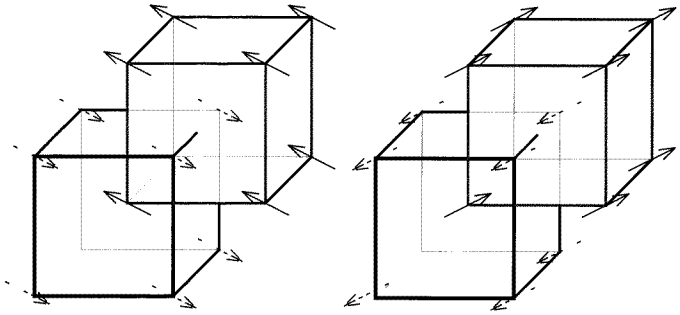

Figure 2. A sketch of the computer model. Spins from σ^1- and σ^4-sublattices (left) are artificially separated from spins from σ^2- and σ^3-sublattices (right) for clarity. Spins from one corner of each cube form the unit cell.

four-spin interaction which covers the *plaquettes* extended to the spins within each unit cell, and the interaction constant is $J_4 = J_{\alpha\alpha}(R, R)$ for σ^α with $\alpha = 1, \ldots, 4$.

In such a formulation the model resembles the well known Ising model with four-spin interaction [9]. The purpose of the present work is rather to employ the model to capture some microscopic properties which could be comparable to the experimental data measured for a system like RbSCN or KSCN. We should briefly mention that, besides the complication of the nonuniversal behaviour [9, 11] of those kinds of model, numerous authors found that a first-order phase transition occurs in the system whenever the four-spin interaction is strong enough or even in a system with only first- and second-neighbour interaction [12]. In particular, we must mention the detailed analysis by Bolton and co-workers [13], in which different approaches point to the existence of a first-order transition in the region of strong four-spin coupling. Quite recently, a phase diagram obtained by the cluster-variation method [14] has shown the occurrence of several regions in the parameter space where a first-order phase transition and re-entrant phenomena occur. Most theoretical papers on that model are limited to the two-dimensional version of the system, and as far as we are aware the computational results are also very limited [17].

A detailed mean-field analysis of the Hamiltonian (1) was presented in [4], and the interested reader is asked to refer to this paper. For our purpose, the important facts are that we can introduce the four-component order parameter [4] as follows:

$$\begin{aligned}
\eta_1 &= \tfrac{1}{4}(\langle\sigma^1\rangle + \langle\sigma^2\rangle + \langle\sigma^3\rangle + \langle\sigma^4\rangle) \\
\eta_2 &= \tfrac{1}{4}(\langle\sigma^1\rangle - \langle\sigma^2\rangle - \langle\sigma^3\rangle + \langle\sigma^4\rangle) \\
\eta_3 &= \tfrac{1}{4}(\langle\sigma^1\rangle + \langle\sigma^2\rangle - \langle\sigma^3\rangle - \langle\sigma^4\rangle) \\
\eta_4 &= \tfrac{1}{4}(\langle\sigma^1\rangle - \langle\sigma^2\rangle + \langle\sigma^3\rangle - \langle\sigma^4\rangle)
\end{aligned} \tag{4}$$

where the $\langle\sigma^\alpha\rangle$ are averages over each sublattice. Only two cases of ordering are physically significant. They correspond to $\eta_1 \neq 0$ and $\eta_2 \neq 0$ together with $\eta_3 = \eta_4 = 0$. Here, $\eta_1 \neq 0$ corresponds to antiferroelectric ordering, while $\eta_2 \neq 0$ corresponds to ferroelectric ordering. Depending on the sign of the interaction constant J_1, the ground state of the model is ferroelectric or antiferroelectric. On the other hand, a negative four-spin interaction J_4 can move the critical temperature to 0 K only if $J_4 > -(J + \frac{4}{3}J_1)$.

Within the mean-field approximation it was shown [4] that the present model possesses a first-order phase transition whenever the four-spin interaction is strong enough. Although a mean-field treatment of the model yields a proper description of quantities such as the susceptibility and the diffuse scattering intensity over a wide range of temperature around the phase transition, it neglects any microscopic effects, which could be crucial in the disordering processes (see, e.g., [7]). In particular, it does not describe the anomalous temperature behaviour of the correlation length below T_c as measured for KSCN [7] and RbSCN [6].

3. Results

The Monte Carlo simulations were performed on a three-dimensional $L \times L \times L$ lattice with periodic boundary conditions. The linear sizes of the model extended from $L = 15$ to $L = 36$ unit cells, with the total number of spins $N = 4L^3$ ranging from 13 500 to 186 624 for the largest lattice. The standard formulation of Metropolis sampling was applied with up to 0.8×10^6 MC steps per spin for each temperature in the critical region. For each temperature, 50 000 sweeps were rejected, and the remaining data were recorded in intervals ranging from 20 to 100 sweeps for the largest lattice. The thermodynamic averages for the order parameter and internal energy were calculated as statistical averages over limited numbers of configurations

for which the system was sampled. Thermodynamic response functions were calculated in the standard way from fluctuations.

Since the numerical calculations were made for finite systems, one has to perform a basic finite-size scaling to obtain any insight into the thermodynamic behaviour. According to the finite-size scaling theory, the free energy of the system is given by the scaling *ansatz*

$$F(L,T) = L^{-\Psi} F^0(L^{1/\mu} t).$$

The finite-size scaling of the free energy leads to the scaling relations for the bulk properties. An additional problem appears if one has to determine precisely the nature of the phase transition, i.e., first versus second order. In the first stage we performed the simulations for the limiting case of $J_1 = J_4 = 0$. For these parameters the system should be equivalent to four independent Ising lattices. Indeed, the system undergoes a phase transition at $T_c = 0.22(1)$ and the order parameter exponent evaluated for this case was $\beta = 0.32(1)$ [15], which within the accuracy of our simulations allows us to place the limit case of the model in the 3D Ising universality class.

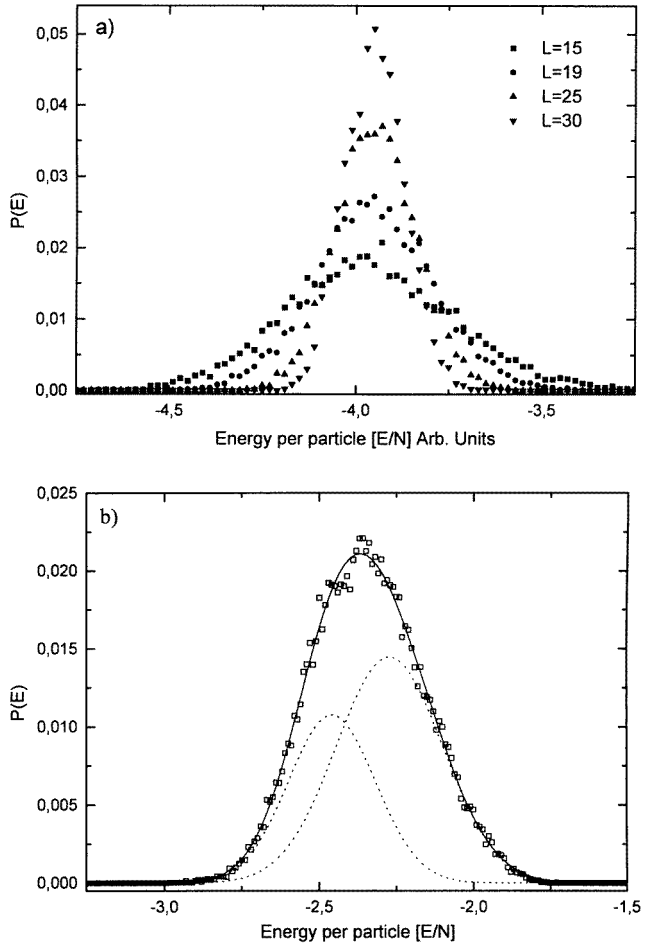

Figure 3. (a) The energy per spin distribution for different lattice sizes and the temperature $T = 0.97T_c$. (b) The energy distribution at $T = 0.995T_c$ together with a fitted double-Gaussian distribution. The two overlapping Gaussians are shown for clarity. The curve is a guide to the eyes.

For this case the phase transition is of second order. Since we are interested in a regime where the system possesses a first-order phase transition which is close to continuous—i.e., near the tricritical point—we have chosen the following parameters for the rescaled Hamiltonian H/J: $J_1/J = 0.5$ and $J_4/J = 2.0$. For this *ansatz* we obtained the following results. For a finite system at a certain temperature, the energy per particle does not have a Dirac delta distribution, but a Gaussian one instead. Such energy distributions can be described by [16]

$$P(E) = \frac{A}{\sqrt{C}} \exp\left(\frac{(E - E_0)^2 L^d}{2k_B T^2 C}\right). \tag{5}$$

C is the specific heat and d the dimensionality of the system. The width of the peak decreases with increasing system size. The energy distribution obtained from the present simulation is depicted in figure 3(a). One can easily see the expected behaviour, and the calculated exponent is equal to $x = 2.96$, which is fairly close to $x = d = 3$. The first-order phase transition is characterized by the phase coexistence close to the transition point. This results in a double

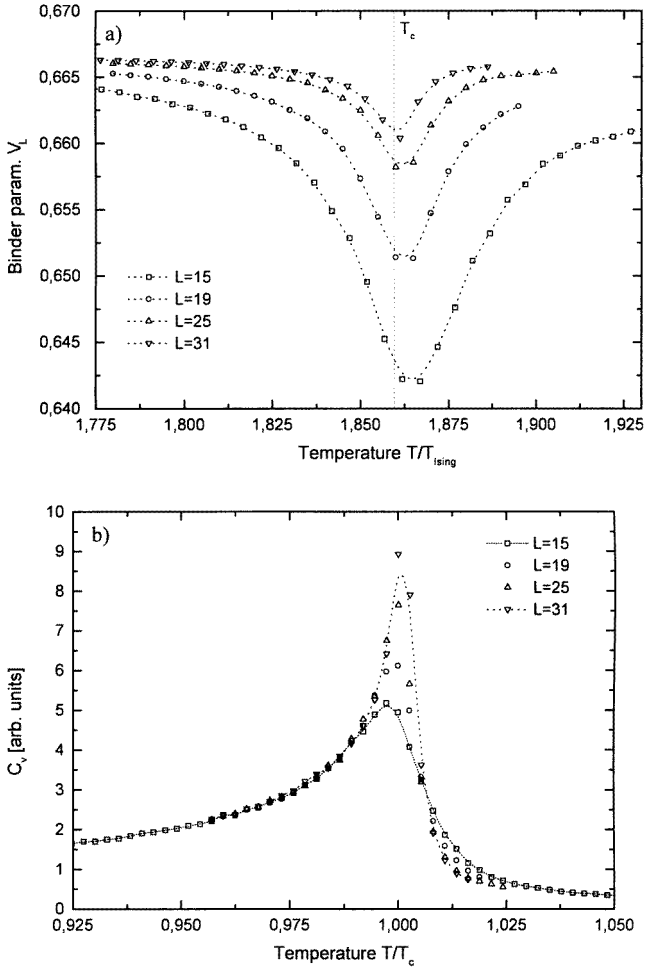

Figure 4. (a) The temperature dependence of the Binder parameter V_L. The transition temperature is compared to the 3D Ising one. (b) The specific heat C_V for different lattice sizes. The curves are guides to the eyes.

peak of the energy distribution close to T_c. In our simulations, the energy distribution in the vicinity of transition point can be well fitted by two Gaussians (see figure 3(b)). The energy ratio between the low- and high-temperature phases estimated from fits equals $E_1/E_2 = 0.05$ which is indeed small, but still nonzero. The small energy *barrier* between phases admits a *weakly* first-order phase transition, which is very close to the tricritical point. To determine the nature of the phase transition and the transition temperature, we used the standard method based on the scaling behaviour of the so-called Binder parameter, which is defined as [17]

$$V_L = 1 - \frac{\langle E^4 \rangle_L}{3\langle E^2 \rangle_L^2}. \tag{6}$$

The Binder parameter has no specific physical meaning; however, it is very useful in the simulations, since it behaves differently for first- and second-order phase transitions. In the case of first-order transitions, the Binder parameter possesses definite minima at T_c equal to [16]

$$V_L(T_c) = 1 - \frac{2(E_+^4 + E_-^4)}{3(E_+^2 + E_-^2)^2}.$$

For the present set of parameters, V_L should approach the value $V_L(T_c) = 0.665$. Far away from T_c, the limit value is $V_L = \frac{2}{3}$. The scaling property of V_L is presented in figure 4(a), where one can see good agreement with the data from the energy distribution. The sharp minimum at T_c indicates that the phase transition is of first order (weak and broad minima are expected for the second-order transitions). The specific heat was calculated as

$$C/k = \beta^2(\langle E^2 \rangle - \langle E \rangle^2)/V$$

and is presented in figure 4(b). With increasing system size, the peak narrows and its height increases; however, the asymmetry with respect to T_c does not vanish.

3.1. Experimental and simulation data

The order–disorder phase transition in RbSCN was previously investigated with diffuse scattering techniques—for details see [6]—and using birefringence measurements. The

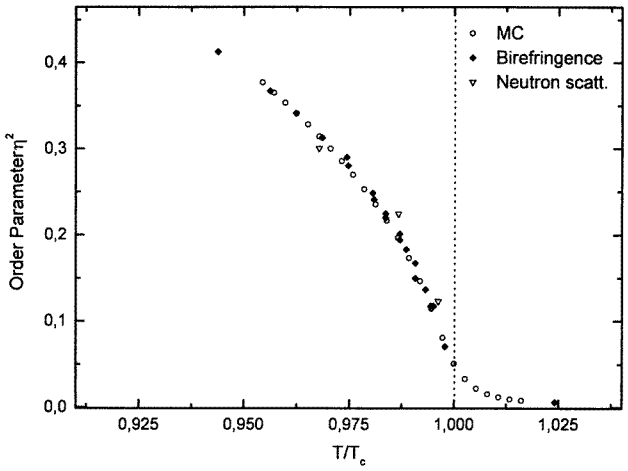

Figure 5. Comparison of the order parameter temperature dependence. ▽: neutron data; ♦: the birefringence; ○: MC points.

temperature dependence of the birefringence was measured with a tilting compensator [18]. Figure 5 shows the temperature dependence of the Bragg intensity of the superlattice reflections normalized to the birefringence data Δn_{ab}. One should notice that both quantities vanish in the tetragonal high-symmetry phase. It can be shown that they are both proportional to the square of the long-range-order parameter η, i.e. $I_B(q_c) \propto \eta^2$ and $\delta n_{ab} = n_a - n_b \propto \eta^2$ [1]. The temperature dependence of the order parameter η_1, which is presented in figure 5, was obtained for simulations for a system with $L = 27$ unit cells, and rescaled for comparison with the experimental points. The rounding at T_c is due to the finite size of the system. The good agreement between the experimental and numerical points encouraged us to analyse the fluctuation behaviour of the system also. We used a simple cluster accounting based on decomposing the spin configuration into a Swendsen–Wang (multiple) cluster [15] to determine the sizes of the ordered regions below T_c. All of the unit cells were divided into

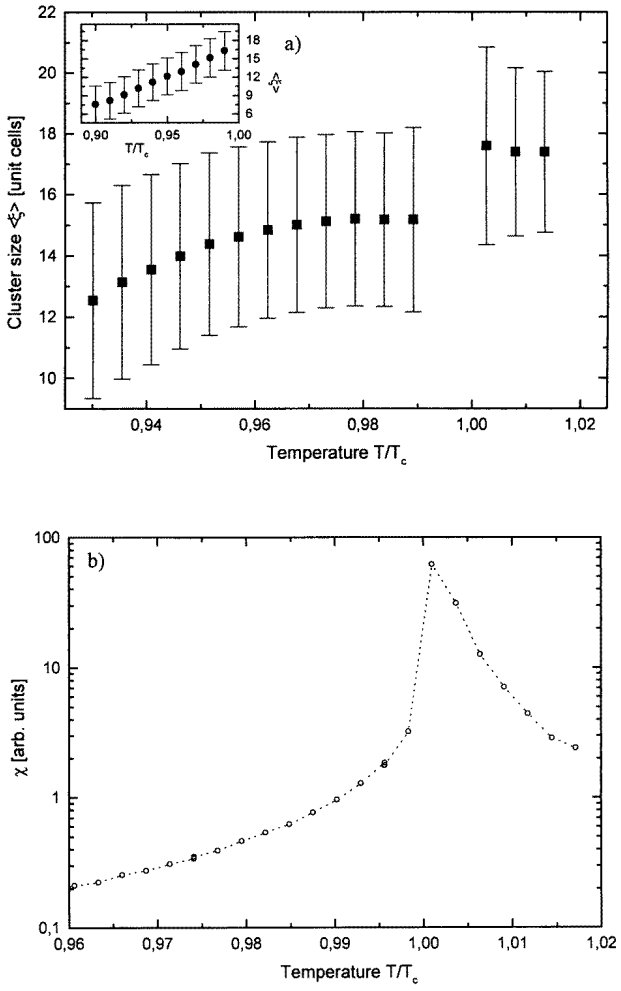

Figure 6. (a) The average size $\langle \xi \rangle$ of the clusters of symmetry different to that of the primary matrix for temperatures below T_c. The inset shows $\langle \xi \rangle$ obtained for the coupling $J_4 = J_1 = 0$. (b) The temperature dependence of the order parameter susceptibility ξ. The curve is a guide to the eyes.

clusters according to the value of the local order parameters η_1 and η_2. Then the volumes of the clusters were sorted into a histogram. The procedure was applied throughout the whole run for each temperature, and the histograms were then averaged. As a result we obtained a distribution of locally ordered regions, which is approximated by a Gaussian. Then we calculated the temperature dependence of the average size $\langle\xi\rangle$ of clusters below T_c, which is presented in figure 6(a). The average size for the limit case ($J_1 = J_4 = 0$) is presented in the inset. In contrast to the monotonic increase of $\langle\xi\rangle$ with temperature for the Ising system ($J_1 = J_4 = 0$), the average cluster size saturates well below T_c for $J_1 \neq J_4 \neq 0$. Figure 6(b) shows the temperature dependence of the order parameter susceptibility $\chi(T)$. According to the fluctuation-dissipation theorem, χ_η is proportional to the diffuse scattering intensity $I_d(q_c)$. In contrast to the cluster size, $\chi_\eta(T)$ increases for $T \to T_c^-$ and $T \to T_c^+$, and exhibits a jump at T_c.

4. Conclusions

We adapted the compressible pseudospin model of the order–disorder phase transition in RbSCN to study microscopic processes of disordering in the vicinity of the transition point. In such a model the influence of the homogeneous elastic strains is equivalent to the effective four-spin interaction. In our Monte Carlo simulation, three-dimensional geometry was used. For the present choice of parameters, the inclusion of next-nearest neighbours and the four-spin interaction results in a first-order phase transition. In the vicinity of T_c, finite-size scaling analysis indicates a very small energy difference between the configurations of the two phases, i.e. the system is very close to a tricritical point. The set of parameters applied in the simulations leads to a fairly good representation of the behaviour of the experimentally measured temperature dependence of the order parameter for RbSCN. The analysis of the distribution of ordered precursor clusters at temperatures below T_c indicates that the average size of the fluctuations increases at temperatures starting from $T = 0.9T_c$, then saturates for temperatures above $T = 0.96T_c$. In contrast, the calculated order parameter susceptibility increases monotonically when approaching T_c from below and displays a jump at T_c, as expected for a first-order phase transition. In fact, the present MC simulations describe the diffuse neutron scattering data for RbSCN and KSCN very well. For both crystals the diffuse neutron scattering intensity $I_d(q_c)$ ($\propto\chi_\eta$) increases when approaching T_c from below, whereas its width w ($\propto\langle\xi^{-1}\rangle$) remains constant. From the 3D MC simulations presented here, and from recent 2D MD simulations, we can conclude that inhomogeneous elastic strain interactions are responsible for the stabilization of the precursor clusters in KSCN and RbSCN. However, it is difficult to explain such behaviour in terms of an analytic model. For example, in Landau–Ginzburg models the temperature dependencies of the order parameter susceptibility $\chi_\eta(q)$ and the correlation length ξ ($\propto$ size of the precursor clusters) are coupled, i.e. $\chi(q_c) \propto \xi^2$, and both quantities increase with increasing temperature below T_c. Therefore, at present we cannot give a definite answer as regards the exact mechanism for this strong suppression of the correlation length below T_c.

Acknowledgments

The present work was supported by the Fonds zur Förderung der wissenschaftlichen Forschung in Austria (Project No P 12226-PHY) and ÖAD Project No 4/98. One of the authors (ZŁ) would like to acknowledge the warm hospitality extended to him during his stay at the University of Vienna.

References

[1] Schranz W 1994 *Phase Transitions* **51** 1
[2] Tröster A 1999 Application of perturbative methods to a model of phase transitions in cubic crystals *PhD Thesis* University of Vienna
[3] Strukov B A and Levanyuk A P 1998 *Ferroelectric Phenomena in Crystals. Physical Foundations* (Berlin: Springer)
[4] Schranz W, Warhanek H, Blinc R and Žekš B 1989 *Phys. Rev.* B **40** 7141
[5] Blasko O, Schwarz W, Schranz W and Fuith A 1991 *Phys. Rev.* B **44** 9159
[6] Blasko O, Schwarz W, Schranz W and Fuith A 1994 *J. Phys.: Condens. Matter* **6** 3469
[7] Blasko O, Schranz W, Fally M, Krexner G and Łodziana Z 1998 *Phys. Rev.* B **58** 8362
[8] Łodziana Z and Parliński K 1997 *Ferroelectrics* **191** 65
[9] Baxter R J 1971 *Phys. Rev. Lett.* **26** 832
[10] Lee F, Chen H H and Wu F Y 1989 *Phys. Rev.* B **40** 4871
[11] Kadanoff L P and Wegner F J 1971 *Phys. Rev.* B **4** 3989
Ditzian R V 1972 *Phys. Lett.* A **42** 67
Oitmaa J and Gibberd R W 1973 *J. Phys. C: Solid State Phys.* **6** 2077
Minami K and Suzuki M 1993 *Physica* A **195** 457
[12] Morán-Lopez J L, Aguilera-Granja F and Sanchez J M 1994 *J. Phys.: Condens. Matter* **6** 9759
[13] Bolton H C and Lee B 1970 *J. Phys. C: Solid State Phys.* **3** 1433
Lee B S and Bolton H C 1971 *J. Phys. C: Solid State Phys.* **4** 1178
Bolton H C, Lee B S and Millar J W L 1972 *J. Phys. C: Solid State Phys.* **5** 2445
[14] Buzano C and Pretti M 1997 *Phys. Rev.* B **56** 636
[15] Binney J J, Dowrick N J, Fisher A J and Newman M E J 1992 *The Theory of Critical Phenomena And Introduction to the Renormalization Group* (Oxford: Clarendon)
[16] Mutry S S, Challa, Landau D P and Binder K 1986 *Phys. Rev.* B **34** 1841
[17] Landau D P 1980 *Phys. Rev.* B **21** 1285
Binder K and Landau D P 1980 *Phys. Rev.* B **21** 1941
[18] Fuith A, Schranz W and Łodziana Z 1999 to be published